Journal of Pharmaceutical Innovation (2024) 19:45
https://doi.org/10.1007/s12247-024-09850-w

ORIGINAL ARTICLE

Fluconazole-Niosome-Laden Contact Lens: A Promising Therapeutic Approach for Prolonged Ocular Delivery and Enhanced Antifungal Activity

Ghada E. Yassin[1,2] · Mai A. Amer[3] · Islam M. Mannaa[2] · Maha Khalifa Ahmed Khalifa[1]

Accepted: 4 July 2024

Abstract

Background Traditional routes of administration of fluconazole such as eye drops have a low therapeutic efficacy due to insufficient bioavailability.

Purpose Herein, a fluconazole noisome-laden contact lens was prepared to control and prolong the drug release and improve its bioavailability.

Methods Two methods have been used to prepare fluconazole niosomes: solvent injection method and thin film hydration method utilizing span 60 and cholesterol mixture. Subsequently, formulations were optimized using three factors and a two-level factorial design and were subjected to in-vitro characterization for the size of niosomes, zeta potential, entrapment efficiency percent, and cytotoxicity study. The optimized fluconazole niosomes were further entrapped in contact lenses by the soaking method and were evaluated according to in-vitro release profile, and antimicrobial activity.

Results The results revealed that the investigated fluconazole niosomes are of nano-size ranging from 228.2 to 769.2 nm with zeta-potential values between − 18.1 and − 60.2 mV. The entrapment efficiency percentage ranged from 51.3 to 75%. Fluconazole was released from fluconazole noisome-laden contact lens and showed a prolonged release up to 48–72 h with a cumulative release of 79.62%. Statistical analysis showed that fluconazole-noisome-laden contact lenses have a significant impressive fungal adhesion reduction as compared to fluconazole-laden contact lenses.

Conclusion Fluconazole noisome-laden contact lenses are a promising therapeutic way for effective and prolonged treatment of ocular fungal infection.

Keywords Fluconazole · Contact lenses · Noisome · Optimization · Antifungal activity · Ocular delivery

Introduction

Ocular fungal infections affect a wide range of populations. The most common dosage forms used for ocular drug delivery are topical eye drops, ointments, gels, or emulsions; they are mostly used to treat ocular surface and anterior segment diseases. It is the most preferred method due to the ease of drug administration and low cost [1]. Following topical administration, several drawbacks affect the bioavailability of such formulations; these factors are known as precorneal factors and include nasolacrimal drainage, blinking, tear film, tear turnover, and induced lacrimation [2]. These results in poor ocular bioavailability (< 5%) due to short drug residence time [2, 3]. The frequency of dosing (4 times/day) affects the routine lifestyle of patients [4, 5]. As a result, research has recently focused on creating a unique

✉ Maha Khalifa Ahmed Khalifa
Mahakhalifa.pharmg@azhar.edu.eg; Mahakhalifa11ahmed@gmail.com; mahakhalifa.ahmed@yahoo.com

[1] Department of Pharmaceutics & Pharmaceutical Technology, Faculty of Pharmacy Girls, Al- Azhar University, Cairo, Egypt

[2] Department of Pharmaceutics and Industrial Pharmacy, Faculty of Pharmacy, October University for Modern Science and Art, Giza, Egypt

[3] Department of Microbiology and Immunology, Faculty of Pharmacy, October University for Modern Sciences and Arts MSA, Giza, Egypt

Published online: 20 July 2024

method or medical device that extends the period that medication remains in the eye, improving the drug's bioavailability and resolving the problems with current dose forms. The possibility of using contact lenses for ocular drug delivery was first discussed by Sedlacek in the mid-1960s [6]. The usage of contact lenses seems to be an advantageous choice because they are versatile, biocompatible, and economical [7]. To provide continuous drug administration, the medication is loaded into the contact lens using a variety of approaches, including the soaking method, drug-loaded nanoparticles, imprinting, drug-polymeric film, and supercritical fluids [3, 8–10].

Mehta et al., 2017 used the electrospinning method to formulate timolol-loaded nanofibers, permeation enhancers were used to coat the external surface of the contact lens [11]. The system showed burst drug release [> 85%] within 24 h. Ciolino et al., 2014 fabricated latanoprost-loaded film in the contact lens by using the method of spin casting, the results showed sustained drug release for one month [12]. Jung et al., 2013 fabricate timolol-propoxylated glyceryl triacylate nanoparticles laden silicon contact lenses for timolol delivery during one month. However, the presence of nanoparticles altered the critical lens properties [13]. Costa et al., 2010 use silicon contact lenses loaded with acetazolamide and timolol by discontinuous supercritical impregnation technology [14]. Puerarin-loaded -cyclodextrin contact lenses were developed by Xu et al. in 2010 and demonstrated an improvement in swelling index and tensile strength in addition to high burst release [9]. Thus, several works of literature showed that a sustained effect can be obtained as a result of using therapeutic contact lenses [15–17].

Fluconazole (Flu) is a broad-spectrum triazole antifungal agent used for the treatment of pathogenic fungi, including *C. albicans*. It has a low penetration rate when applied topically and many oral side effects. To overcome the problems of conventional ocular therapy, fluconazole niosomes were developed [18].

Recently, vesicular drug delivery systems (phospholipid vesicles as liposomes and non-ionic surfactant vesicles as niosomes) have been employed in ophthalmology to achieve prolonged drug release and reduce enzymatic drug metabolism at the ocular surface and at the corneal surface, respectively [19]. Vesicles offer the ease of eye drops while allowing the sustained medication action to be maintained at the site of action for a longer period [20]. Niosomes are non-ionic amphiphilic vesicles composed of non-ionic surfactant bilayer compartments that can, contain hydrophilic and hydrophobic pharmaceuticals [21]. Occasionally, charged molecules and cholesterol are added to the solution to boost stability and stiffen the bilayers [22]. In addition, niosomes offer extra benefits over conventional micro- and nano-delivery technologies by enhancing the low bioavailability and penetration through the cornea [23]. According to Carafa et al., 2002, niosomes have advantages over other vesicular systems for topical ocular delivery as they are chemically stable, have low toxicity due to their non-ionic nature, can improve the performance of the drug through better availability, and are non-immunogenic, biocompatible, and degradable [24]. In aqueous conditions, non-ionic amphiphiles self-assemble to generate non-ionic surfactant-based vesicles (niosomes), which finally form closed bilayer structures that can entrap both hydrophilic and lipophilic medicines either in an aqueous layer or in the vesicular membrane, according to Carafa et al. (1998) [25]. According to Kaur et al.'s 2000 study, drug vesicles, which are tiny, spherical particles, can be used to localize and maintain drug activity at its site of action while having the ease of a drop in ocular drug delivery [26].

Thus, the present work aims to encapsulate fluconazole in niosomal vesicles which were then uploaded onto a contact lens for sustaining the drug release, for better drug bioavailability, and for patient compliance improvement.

Material and Method

Material

Cholesterol, span 60, sodium chloride, disodium hydrogen-phosphate, potassium dihydrogen-orthophosphate, sodium dihydrogen-phosphate, and acetone were obtained from Sigma-Aldrich Co., (USA) fluconazole was gifted from SEDICO pharmaceutical corporation, Egypt. A dialysis membrane (MWCO 14000) was purchased from Sigma-Aldrich Co., (USA). All other chemicals and solvents were of analytical grade and obtained from El-Nasr Company for Pharmaceutical Chemicals, Cairo, Egypt.

Methods

Pre-Formulation Studies

Fourier-Transform Infrared Spectroscopy (FTIR) The potential interactions between fluconazole, Span 60, and cholesterol were investigated using FT-IR spectroscopy (IR Prestige 21 Shimadzu, Japan) Fourier Transform Infrared (FTIR) spectroscopy was used to determine the compatibility of Flu with excipients and to ensure the absence of any interactions that could affect the drug molecule [27]. The FT-IR analysis of fluconazole, span 60, cholesterol, and a physical mixture of fluconazole, span 60, and cholesterol

was performed with a resolution of 2 cm^{-1} in the 4000 to 400 cm^{-1} range [28].

Differential Scanning Calorimetry (DSC) The DSC test was used to understand the thermal behavior of drugs and other components used in the niosomes as well as to record any melting point changes between the pure drug and the formulation's excipients [27]. The thermograms were created using a DSC-50 thermal analyzer (Shimadzu, Kyoto, Japan). Five mg of samples were sealed in aluminum pans, the samples were subjected to be heated at 10 °C/min ranging from 0 to 400 °C. DSC was done on fluconazole, span 60, cholesterol, and a physical mixture of fluconazole, span 60, and cholesterol [28].

X-ray Diffraction Scanning (XRD) The XRD test was used to investigate the crystalline structure of fluconazole and excipients. X-ray diffraction (XRD) patterns were generated by CuK radiation that were collimated by a 0.08° diverging slit and a 0.2° receiving slit and scanned at a rate of 2.4°/min across a 5-100° range. The diffractometer was employed (Philips, Holland, PW 3710). The apparatus worked at 40 kV voltage and 30 mA current. The XRPD analysis was carried out on fluconazole, span 60, cholesterol, and a physical mixture of fluconazole, span 60, and cholesterol [29].

Statistical Optimization

For optimizing the niosomes formulation (2^3) factorial design was used to clarify the impact of the formulation factors. The studied independent variables included drug amount (X_1), preparing method (X_2), and span 60/Cholesterol ratio (X_3). Sixteen experimental runs were performed by Design-Expert software (version 7.0.0 software, State-Ease Inc., USA) as seen in Table 1. The response parameters in this study were particle size (PS) (Y_1), zeta potential (ZP) (Y_2), and percentage of entrapment efficiency (EE%) (Y_3).

The best-fitting model for each response was chosen according to the computed adequate precision ratio, as well as the predicted and adjusted determination coefficients. The significance of formulation factors was estimated by analysis of variance (ANOVA) at $p < 0.05$. Tables 1 and 2 show the design matrix.

Table 1 D-optimal design factors, levels, and target constraints for the niosomes

Independent factors	Levels	
	Low level	High level
Drug amount	20 mg	40 mg
Preparation method	B1*	B2**
Span 60 / Cholesterol ratio	1:2	2:1
Response	**Constraints**	
Y_1: Particle size (PS)	Minimize	
Y_2: Zeta potential (ZP)	Maximize	
Y_3: Percentage of entrapment efficiency (EE%)	Maximize	

* B1: Injection method

** B2: Thin film hydration (THF) method

Formulation of Fluconazole Niosomes According to the D-optimal Design

Solvent Injection Method [30]

Niosomes were prepared using a modified solvent injection technique. Cholesterol and span 60 were carefully weighed and dissolved in dichloromethane (20 ml) according to ratios and weights in Table 1. This lipid solution was then used to dissolve fluconazole (20 or 40 mg). The obtained solution was injected at a rate of 1 ml/min through a pump syringe into a beaker containing 4 ml of phosphate buffer (pH 7.4). The solution was kept at 60-65°C and slowly agitated. The vaporization of chloroform which was slowly injected into the phosphate buffer led to niosomes formation. These niosomes were refrigerated at 4°C until ready to use [31].

Thin Film Hydration (THF) Method [32]

Cholesterol, span 60, and fluconazole (20 or 40 mg) were added in a round bottom flask and dissolved homogeneously in 20 ml of dichloromethane. The solvent is then entirely evaporated by introducing it to a rotary vacuum evaporator at 60°C and a speed of 100 RPM, leading to the formation of a thin layer on the flask's inner surface. Then rehydrate the formed film in an aqueous solution for 30 min with phosphate buffer saline (PBS), which is usually used to encapsulate the drug. Noisomes of varying sizes were generated once rehydration was completed then they were subjected to a probe sonicator for 3 min.

Characterization of Noisome

Particle Size, PDI, and Zeta Potential

One ml of fresh formulations was diluted with 9 ml of deionized water and vortexed. The size, zeta potential, and PDI of the prepared dispersions were then measured using a Malvern Zetasizer (Malvern Instruments Ltd., United Kingdom). Measurements were made in triplicate at room temperature (25 °C). The mean and standard deviation of all values were given.

Table 2 Composition and the observed responses of the design

	Independent factors			Dependent variables*			PDI
Run	A: Drug Concentration	B: Method of preparation	C: span: cholesterol ratio	*P*.S.	Zeta pot.	EE	
	mg			nm	mV	%	
1	40	(B2) TFH	2:1	228.2 ± 2.04	34.3 ± 0.15	58.4 ± 1.05	0.58 ± 0.1
2	20	(B1) Injection	2:1	254.2 ± 1.99	44.7 ± 0.26	69 ± 2.07	0.658 ± 0.08
3	40	(B1) Injection	2:1	769.2 ± 1.05	46.4 ± 0.81	74 ± 0.066	0.6 ± 0.05
4	20	(B2) TFH	2:1	635.3 ± 2.05	54.3 ± 1.22	70.8 ± 1.08	0.8 ± 0.06
5	20	(B1) Injection	1:2	269.9 ± 3.4	47.3 ± 0.98	64 ± 1.6	0.483 ± 0.01
6	40	(B2) TFH	1:2	494.9 ± 4.56	47.3 ± 0.85	64 ± 1.74	0.565 ± 0.09
7	20	(B2) TFH	1:2	269.6 ± 2.07	46.1 ± 0.78	51.3 ± 1.25	0.414 ± 0.14
8	40	(B1) Injection	1:2	450.6 ± 4.32	18.1 ± 0.26	62 ± 2.66	0.496 ± 0.17
9	20	(B1) Injection	1:2	275 ± 1.26	50.2 ± 1.37	69 ± 1.98	0.723 ± 0.2
10	40	(B2) TFH	2:1	235 ± 3.55	29 ± 0.91	60.2 ± 1.56	0.43 ± 0.07
11	40	(B1) Injection	1:2	455 ± 4.78	20.3 ± 0.78	63 ± 2.8	0.413 ± 0.17
12	20	(B2) TFH	2:1	642 ± 3.79	68 ± 2.46	72.6 ± 3.79	0.7 ± 0.07
13	20	(B1) Injection	2:1	260 ± 1.77	48 ± 0.98	74 ± 4.35	0.588 ± 0.3
14	40	(B2) TFH	1:2	485 ± 6.59	42 ± 1.25	75 ± 3.99	0.923 ± 0.09
15	20	(B2) TFH	1:2	274 ± 3.98	48.1 ± 0.69	55 ± 2.89	0.558 ± 0.1
16	40	(B1) Injection	2:1	775 ± 3.77	48 ± 1.0	75 ± 1.89	0.484 ± 0.08

Data presented as mean($n = 3$) ± SD.

*: EE%: percentage of entrapment efficiency; PS: particle size; ZP: zeta potential: PDI: polydispersity index

Entrapment Efficiency Percentage

The fraction of the administered drug that is entrapped by the noisome is known as entrapment efficiency (EE %) [33]. Separation of fluconazole-loaded niosomes from the un-entrapped fluconazole was performed using cooling centrifugation [18, 34]. Entrapment efficiency was calculated by centrifuging one ml of the suspension of niosomes at 12000 rpm for 30 min and 4 °C for 1 h using a cooling centrifuge (OptimaTM MAX-XP Ultracentrifuge; Beckman Instruments); the supernatant containing the unentrapped fluconazole was then taken and measured for the fluconazole amount at 260.5 nm using a UV spectrophotometer (V-630, Jasco, Japan) [33]. The following equation was used to calculate the EE%:

$$\begin{aligned} \mathrm{EE}\,\% &= \text{Total amount of Flu} \\ &- \text{amount of FLU in supernatent (un entrapped)} \\ &/\text{Total amount of Flu} \times 100 \end{aligned} \quad (1)$$

All measurements were made in triplicate at room temperature (25 °C). The mean and standard deviation of all values were given.

Optimization of Formulation Variables and Model Validation

The optimized fluconazole niosomes formula was selected according to the desirability tool, which permitted the investigation of each response simultaneously. Choosing the fluconazole niosomes selected formula based on fabricating vesicles with minimum particle size, maximum entrapment efficiency, and maximum zeta potential. The optimized formula was evaluated and its responses were compared to the predicted values. The model was validated by calculating the percentage error.

Transmission Electron Microscopy (TEM)

Flu-NS optimized formula morphology was observed using (EM (JEM-2100, JEOL, Japan). For this purpose, a drop of diluted dispersion and a drop of 2% w/v phosphotungstic acid were added to a carbon-coated copper grid (400 mesh). After drying the sample, they were seen and photographed using a Philip CM 120 Bio-Twin TEM (Philip Electron Optics BV, Netherlands).

Cytotoxicity Test for the Optimized Formulae

Cell Culture

Normal Mouse Endothelial Cell line (C-166) obtained from Nawah Scientific Inc., Mokatam, Cairo, Egypt) was used. The cells were routinely maintained for culture in DMEM media that was supplemented with streptomycin (100 mg/ml), penicillin (100 unit/ml), and inactivated fetal bovine serum (10%) at 37° C in, a CO_2 atmosphere (5%v/v).

Sulforhodamine B (SRB assay) was used to assess cell viability [35, 36]. Briefly, 1 hundred microliters of the cell suspension (5×10^3 cells) were transferred to 96-well

culture plates and incubated overnight. Following, the cells were exposed to 100 µl of media supplemented with the control, Flu-Nio, and Flu solution (10 µg/ml) or to vehicle control and incubated for 24 h. Cell fixation was then done by medium removal and adding 150 µl of 10% trichloroacetic acid (TCA), followed by incubating for 1 h at 4 °C. TCA was washed five times using distilled water. Staining was done by adding 70 µl SRB solution (0.4% w/v), followed by incubation at room temperature for 10 min in a dark environment. Plates were washed thrice using acetic acid (1% v/v) and left for drying. To dissolve protein-bound SRB stain; TRIS (150 µl) at 10 mM was added, followed by colorimetric absorbance measurement at 540 nm using a BMG LABTECH®- FLUO star Omega microplate reader (Ortenberg, Germany) and the percent of cell viability (%) was calculated as follows [37]:

$$Viability\ (\%) = \text{Absorbanceoftreatedcells} / \text{Absorbanceofuntreatedcells} \times 100 \quad (2)$$

Fluconazole Loading on the Contact lens

Loading of Fluconazole Noisome (Flu-Nio) into the Contact Lenses Using the Soaking Method [38]

Two ml of niosomal suspension containing 8 mg fluconazole was used to soak the contact lenses (Maulvi, 2015). The contact lenses were soaked for different time intervals at 4 days and 7 days. After that, the contact lenses were blotted with tissue paper to get rid of the excess of the soaking solution from the contact lenses' surface.

Fluconazole Quantification in the Contact Lenses

The concentration of fluconazole uptaken in the contact lenses was assessed by adding the lenses individually in screw-capped vials having 25 ml of methanol. They were shaken for 2 days at 200 rpm by a shaker for complete Flu extraction. The extracted drug was quantified at 260.5 nm using a UV spectrophotometer (V-630, Jasco, Japan).

Light Transmission

The transparency of the contact lens was measured using a UV-spectrophotometer (V-630, Jasco, Japan) at the wavelength of 600 nm [6]. Distilled water is used to soak the contact lenses overnight to improve the lens flexibility to fit into the cuvette after which light transmission was measured.

In vitro Fluconazole Release Study

In vitro release of Flu from Flu-Nio-laden contact lenses was evaluated by the dialysis bag method using pure fluconazole as a control [38]. Flu-NS contact lenses equivalent to 3 mg of Flu and the same weight of free Flu were entrapped in a dialysis bag (MWCO 14000 Da; dialysis tubing cellulose membrane, Sigma-Aldrich) with 2 ml of simulated tear fluid (STF) (pH = 7.4) in a glass vial to mimic the in vivo conditions of tear turnover [39]. They shaked in an incubator shaker at 100 RPM and 35 °C to simulate eye blinking conditions. At time intervals of 0.5, 1, 2, 3, 24, 48, 54, and 72 h, 2 ml of the sample was withdrawn from the dissolution medium. The emulated tear fluid was changed at these intervals with the same quantity of fresh emulated tear fluid to maintain sink conditions. After appropriate dilution, the amount of fluconazole was measured using a spectrophotometer at 260.5 nm. The previously constructed calibration curve was used to calculate the mean cumulative % of dug released and was plotted against time. Each test was performed in triplicate ($n = 3$). Furthermore, the in vitro drug release data of fluconazole from the optimized Flu-Nio-laden contact lenses was investigated and evaluated by fitting to zero-order, first-order, and Higuchi models to explain the mechanism of drug release.

Antimicrobial Activity Study

Bacterial Strains and Culture Conditions

Candida albicans (ATCC® 10231) was used in this study. The stock solution was preserved in glycerol stock at -20 ºC, routinely cultured aerobically into 10 ml of Sabouraud dextrose broth (SDB), and incubated overnight at 37ºC.

Determination of Antifungal Susceptibility (Kirby-Bauer Method)

The susceptibility of *C. albicans* (ATCC® 10231) to Flu-Nio laden lenses, Flu-laden contact lenses, Flu-Nio disc, and Flu disc was determined in vitro, using the disc diffusion method according to the Clinical and Laboratory Standards Institute (CLSI) guidelines [40]. From a pure culture, 5–6 colonies of the organism were transferred to a test tube containing 0.9% saline. The suspension turbidity was adjusted to be equivalent to 0.5 McFarland Standard. Mueller-Hinton agar (MHA) (Lab M, Lancashire, UK) was poured in plates at a depth of 5 to 6 mm and the plates were air dried for 30 min. The adjusted culture was swabbed on plates in three different directions to ensure complete coverage of the agar surface. Fluconazole and fluconazole noisome-laden contact lenses were placed aseptically using sterile forceps to

the surface of the inoculated plates and their produced zone of inhibition is compared to Flu-Nio and Flu discs that were also placed on the surface of the medium. The plates were incubated at 37oC for 24 h. Flu-Nio and Flu discs are prepared by impregnation of sterile filter paper discs with the desired concentration of Flu-Nio and Flu solutions, respectively. Zones of complete inhibition were measured in mm [41]. Each experiment was performed in triplicates.

Determination of the Fungal Adhesion

Overnight cultures of *C. albicans* (ATCC® 10231) were adjusted to a turbidity equivalent to 10^8 colony forming unit (CFU)/ ml, followed by ten folds serially diluted to 10^3 CFU/mL and the adjusted turbidity was used for the adhesion assay [42].

Fluconazole and Flu-Nio-laden contact lenses were washed twice with PBS (1 ml) and then were transferred into 24-well tissue culture plates containing 1 ml of the adjusted fungal suspension and incubated at 37ºC for 24 h. Lenses were washed thrice using PBS and vortexed for 30 s to remove loose cells. Contact lenses were further transferred into 2 mL of PBS and placed in test tubes. The test tube was allowed to vortex at a maximum speed for 1 min to detach the cells adhered to the lenses. Following log serial dilution, plating was done on SDA [43] for the cell counts. After overnight incubation at 37ºC, CFU was quantified and measured as CFU/lens. The fungal adhesion on Flu-Nio-laden contact lenses was compared with the control lenses, and the reduction of fungal adhesion was determined accordingly. The experiment was done in triplicates [42].

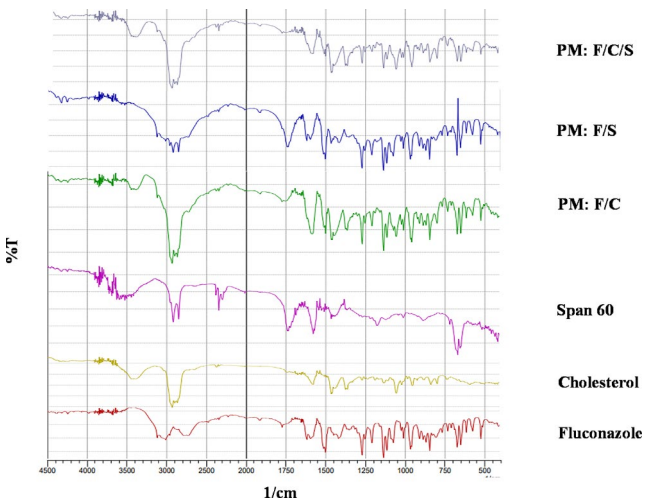

Fig. 1 FTIR spectrum of fluconazole, cholesterol, span 60, physical mixture of fluconazole and cholesterol (PM: F/C), physical mixture of fluconazole and span 60 (PM: F/S), and physical mixture of fluconazole, cholesterol, and span 60 (PM: F/C/S)

Determination of the Inhibition of *C. Albicans* Growth

Following the fungal adhesion assay, fungal growth in the culture suspensions from each treated or control lens was examined by plating out. Following log serial dilution, counting the remaining cells in culture solutions [42]. Following log serial dilution, plating was done on SDA plates and incubated overnight at 37ºC. CFU on the plate was counted and calculated as CFU/ml. The remaining viable *C. albicans* on fluconazole and Flu- Nio-laden contact lenses were compared with control lenses, and the remaining viable fungi were calculated accordingly. The experiment was done in triplicates.

Results and Discussion

Pre-Formulation Studies

Fourier-Transform Infrared Spectroscopy (FTIR)

FTIR was used to study the interactions of fluconazole, cholesterol, span 60, physical mixture of fluconazole and cholesterol (PM: F/C), physical mixture of fluconazole and span 60 (PM: F/S), and physical mixture of fluconazole, cholesterol, and span 60 (PM: F/C/S). The results are shown in Fig. 1. Fluconazole shows six characteristic peaks at 1627 cm^{-1} corresponding to the Triazole ring, 3120 cm^{-1} corresponding to the -OH stretching, 1422 cm^{-1}corresponding to the $-CH_3$ bending, and 1292 cm^{-1}corresponding to the bending vibration of the -CH2 group, 1089 cm^{-1} corresponding to (C–OH bond) and 1107 cm^{-1} corresponding to (C–F bond). The same results were obtained by Fatima et al., 2022 and Moraes et al., 2017 [28, 44]. Asymmetrical stretching of the cholesterol's C-H bond was seen at 2941 cm-1, whereas the stretching -OH cholesterol was seen at 3359 cm^{-1} as shown in Fig. 1. Farmoudeh et al., 2020 reported the same results of cholesterol [45]. Span 60 showed aliphatic C-H stretching at 2882 cm^{-1}, $-CH_3$ group stretching at 1458 cm^{-1}, and O-H stretching at 3390 cm^{-1}. At 1744 cm^{-1}, the cyclic five-membered ring's peak in span 60 was noted. The results were matched with Fatehi et al., 2020 and Miatmoko et al., 2021 [46, 47]. The characteristic peak of pure fluconazole has appeared in all physical mixtures with no change. In the three physical mixtures, FTIR showed all the peaks of cholesterol, and/or span 60 at their places confirming the absence of any chemical interactions between them.

Differential Scanning Calorimetry (DSC)

Figure 2 shows the DSC thermogram of Flu, Cholesterol, span 60, Flu/cholesterol physical mixture, Flu/ Span 60

physical mixture, and Flu/Cholesterol/span 60 physical mixture. Flu thermogram reveals endothermic peaks at 101, 146, 360, and 440 and another peak appeared at 246.75 °C. The first peak corresponds to crystal dehydration, and the temperature matches the boiling point of water. The second peak corresponds to the crystals melting point. Finally, the third and fourth peaks correspond to the degradation of fluconazole. The results are in good agreement with Akay et al., 2021 [48]. The melting points of cholesterol were observed at an endothermic peak at 149 °C and 208.1 °C due to degradation and abroad peak at 44.6 C, due to the loss of water molecules as reported by Abd-Elal et al., 2016 [49]. The same results were obtained by Yasam et al., 2016 when studying the DSC thermogram of cholesterol [50]. The main melting peaks of span 60 were observed at 64°C which is matched with El-Ridy et al., 2018 [51]. The results of DSC of the physical mixtures demonstrated that Flu and the excipients melting peaks appeared in their places without undergoing shifting, and with no extra peaks appearing, showing an absence of interaction between Flu and excipients.

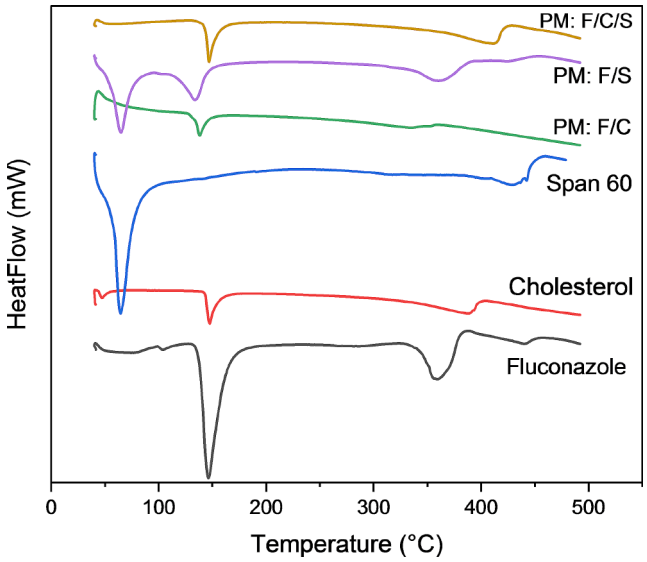

Fig. 2 DSC of fluconazole, cholesterol, span 60, physical mixture of fluconazole and cholesterol (PM: F/C), physical mixture of fluconazole and span 60 (PM: F/S), and physical mixture of fluconazole, cholesterol, and span 60 (PM: F/C/S)

X-Ray Diffraction Scanning (XRD)

The characteristic (XRD) patterns of fluconazole, Cholesterol, span 60, Physical mixture of fluconazole and Cholesterol (PM: F/C), Physical mixture of fluconazole and span 60 (PM: F/S), and Physical mixture of fluconazole, Cholesterol, and span 60 (PM: F/C/S) are compared and illustrated in Fig. 3. The diffraction pattern of fluconazole showed high-intensity crystallinity peaks at 16.584, 25.652, and 29.30 °2θ. The peak with 100% relative intensity was present at °2θ value of 20.03. These results are similar to that of Modha et al., 2010 [52]. On the other hand, the diffraction pattern of cholesterol showed an intense peak at 12.74, 14.14, 15.65, 16.85, 17.27, and 21.44 (100% relative intensity) and 23.89°2θ [53], while the diffraction pattern of span 60 showed a 100% relative intensity at 21.433 °2θ. When the diffractograms of the physical mixtures and fluconazole were compared, all the characteristic crystalline peaks for

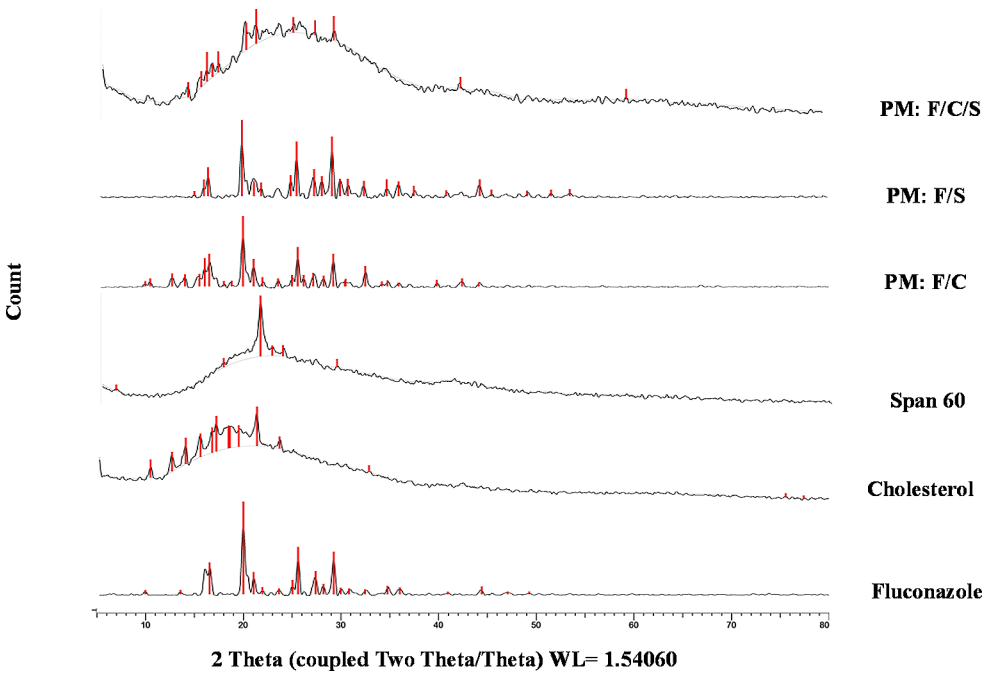

Fig. 3 X-ray diffractograms of fluconazole, cholesterol, span 60, physical mixture of fluconazole and cholesterol (PM: F/C), physical mixture of fluconazole and span 60 (PM: F/S), and physical mixture of fluconazole, cholesterol, and span 60 (PM: F/C/S)

fluconazole could be observed with the same intensity revealing that no changes were made to the fluconazole.

Experimental Design and Optimization of

The goal of the design expert optimization is to study the effect of experimental factors on the formulation's responses. Table 2 shows the factors and the observed responses. The two factors' interactions (2FI) model was the best fitting model for Y_1, Y_2, and Y_3 responses because it has the highest R^2 and the lowest predicted residual error sum of squares.

The Effect of Investigated Variables on Responses

PS

The size of vesicles is an important consideration in the formulation and optimization of nanocarriers. Flu niosomes sizes ranged from 228.2 to 769.2 nm, as appeared in Table 2. Three FI model was significant at ($p < 0.001$), with a regression coefficient (R^2) of 0.9998 according to ANOVA analysis indicating the goodness of fit. Also, there was an agreement (less than 0.2) between the predicted R^2 (0.9990) and the adjusted R^2 (0.9996). The equation that describes the relationship between particle size and formulation factors is:

$$\mathrm{Ps}\,(Y_1) = 423.31 + 63.31A - 15.31B + 51.56C - 110.53AB - 36.32AC - 24.43BC - 119.98ABC \quad (3)$$

Where A, B, and C correspond to X_1, X_2, and X_3 respectively.

The prepared niosomes have a small particle size on the nanoscale with homogenous distribution according to the result of the polydispersity index (PDI). PDI was found to be lower than 0.7 for most formulations. The polydispersity index (PDI) has values less than 0.7, indicating a narrower size distribution, compared to the particles in a wide distribution which tend to aggregate [54]. Figure 4 and Eq. 3, reveal that PS increases significantly with the increased drug amount at ($P < 0.001$) and this result was in great agreement with the previous work done by El-Far et al., 2022 [55] which stated that drug interacts with the surfactant head groups, increases the charge and mutual repulsion of the surfactant bilayers and thus increases vesicle size. The particle sizes are influenced by the surfactant: cholesterol ratio as shown in Fig. 4; Table 2. Cholesterol is a necessary component in the formation of noise. It improves vesicle stability and plays an important role in bilayer packing [56]. Increasing the surfactant: cholesterol ratio to 2:1 reduced the mean diameter of the particles. This result agreed with the previous data, indicating that a decrease in cholesterol caused the vesicle size to decrease [57]. This could be interpreted by the high levels of cholesterol disrupting the niosomal membrane. Because cholesterol is amphiphilic, it

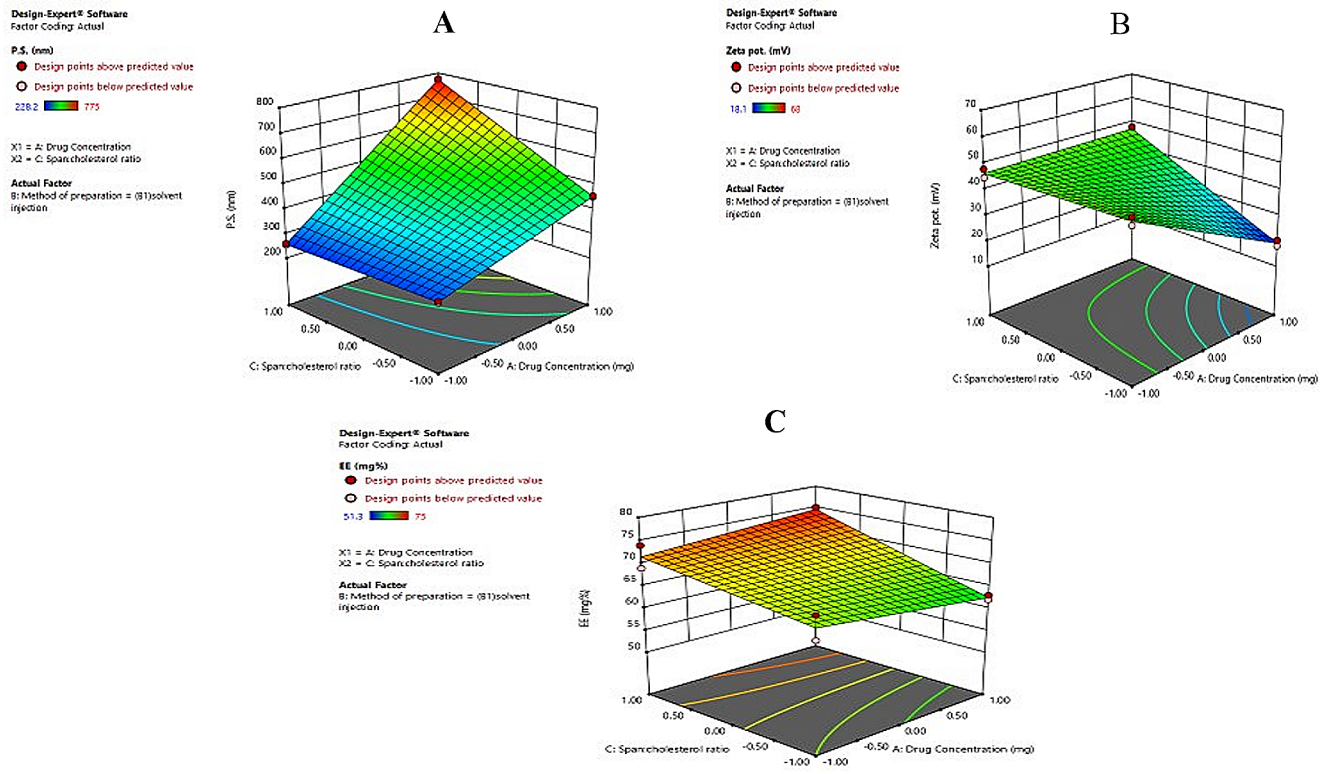

Fig. 4 3D surface response plots showing the impact of the independent variables on (A)PS(Y_1), (B)ZP(Y_2), and (C)EE% (Y_3)

intercalates within the bilayer structure of niosomes by orienting its polar head toward the water-soluble surface and aligning its aliphatic tail parallel to the hydrocarbon chains, forming large vesicles [58]. Teaima et al., 2020 showed that "cholesterol is a stiff, inverted cone-shaped molecule. When hydrated at a temperature above the gel/liquid transition temperature, it can be intercalated between the surfactant's fluid hydrocarbon chains, increasing the size of the vesicle" [59]. The addition of CHO to a membrane increases the membrane bilayer rigidity and reduces water-soluble substance leakage through membranes. Surfactant monomers were closely packed with increasing curvature and decreasing size at low CHO concentrations. On the other hand, at high CHO concentration, and low nonionic surfactant content, the lipophilicity of the bilayer membrane increases (log P of 7.02). Also, it may increase the vesicle radius and create a thermodynamic stable form causing disturbance in the vesicular membrane [60]. Moreover, CHO can remove the vesicle's phase transition temperature peak leading to stabilize the bilayer structure, thereby strengthening the bilayer structures and decreasing bilayer micro fluidity [61]. It was found that the increase in surfactant amount (span 60) and decrease in cholesterol amount resulted in a significant decrease in the particle size as shown in Fig. 4; Table 2. This may be due to the physical characteristic of span 60 as a solid surfactant with low HLB (HLB = 4.7), higher phase-transition temperature (53–57 °C), and surface free energy, which decreases with increasing lipophilicity [56, 62]. The produced niosomes had with larger mean vesicle diameter in the solvent injection method (B1) as compared to the thin film hydration method (B2). These findings were in great agreement with that of Kumar et al., 2013 who investigated the influence of various preparation techniques on the formulation of Diclofenac niosomes [63]. Also, the same findings were obtained by Mujeeb et al., 2017 [64].

ZP

The developed 3FI model for the preparing method factor (Y_2) was significant at ($p < 0.0006$), with a regression coefficient (R^2) of 0.9473 according to ANOVA analysis showing the model is well fit. The predicted R^2 (0.7246) agrees with the adjusted R^2 (0.8946) (less than 0.2). The adequate precision was 13.94 suggesting that the signal was adequate. The equation that describes the relationship between ZP and formulation factors is:

$$\begin{aligned} \mathrm{ZP}\ (Y_2) &= 43.26 - 7.58A + 2.88B + 3.33C \\ &- 0.406AB + 0.418AC - 3.07BC - - 7.18ABC \end{aligned} \quad (4)$$

Where A, B, and C correspond to X_1, X_2, and X_3 respectively. Values were between −18.1 and −60.2 mV in all cases. All the formulations presented negative values of zeta potential due to hydroxyl ions adsorption on the surface of the vesicle by non-ionic surfactants and to the effect of CHO, which produces a negative charge on the vesicle surface [55]. The higher electrostatic repulsion results in higher negative values providing more stability [65]. The thin film hydration method (B2) provided more stable niosomes than that of the injection method (B1). These findings were in great agreement with Mujeeb et al., 2017 [64].

EE%

The EE% of fluconazole niosomes ranged from 51.3 to 75%, as demonstrated in Table 2. Three FI model was significant at ($p < 0.0005$), with a regression coefficient R^2 of 0.9496 according to ANOVA analysis showing that the model is well fit. Also, the predicted R^2 (0.7369 agrees with the adjusted R^2 (0.8994), and the difference is less than 0.2. The equation that shows the relationship between EE% and formulation factors is:

$$\begin{aligned} \mathrm{EE\%}\ (Y_3) &= 66.08 + 0.368A - 2.67B + 3.17C \\ &+ 0.6188AB - 2.72AC - 1.08BC - 4.74ABC \end{aligned} \quad (5)$$

Where A, B, and C correspond to X_1, X_2, and X_3 respectively.

As represented in Fig. 4, increasing the drug ratio resulted in a non-significant increase in the EE% of fluconazole, with p values = 0.5529. A higher surfactant ratio led to a significantly higher EE%, which may be related to span 60 has phase transition temperature (53 °C) which resulted in a decrease in the fluidity and breakage of the bilayer. Also, span 60 has a HLB value of (4.7) with a long C17 chain), which increases its hydrophobic character to be able to hold the hydrophilic drugs inside its core [66]. Previous research has shown that when CHO is used above a certain optimum concentration, it may decrease hydrophilic drugs EE%, the reason may be because of a disruption in the bilayer physical organizational structure, leading to leakage [66].

Selection of the Optimized Flu-Nio

The desirability function was based on the conditions for attaining minimum PS (Y_1), maximum ZP (Y_2), and maximum EE% (Y_3). The Flu-Nio optimized formula was developed by using a fluconazole amount of 20 mg (X_1), solvent injection as a method of preparation (X_2), and a Surfactant: cholesterol ratio of 2:1 (X_3). The optimized formula is predicted to have PS (Y_1) of 257.1 nm, ZP (Y_2) of -46.35 mv as shown in Fig. 5, and EE% (Y_3) of 71.5% achieving 0.747 the highest desirability. In addition, it was evaluated and compared to the observed values. The percentage error was 1.021, 2.52, and 4.67 for PS, ZP, and EE% respectively.

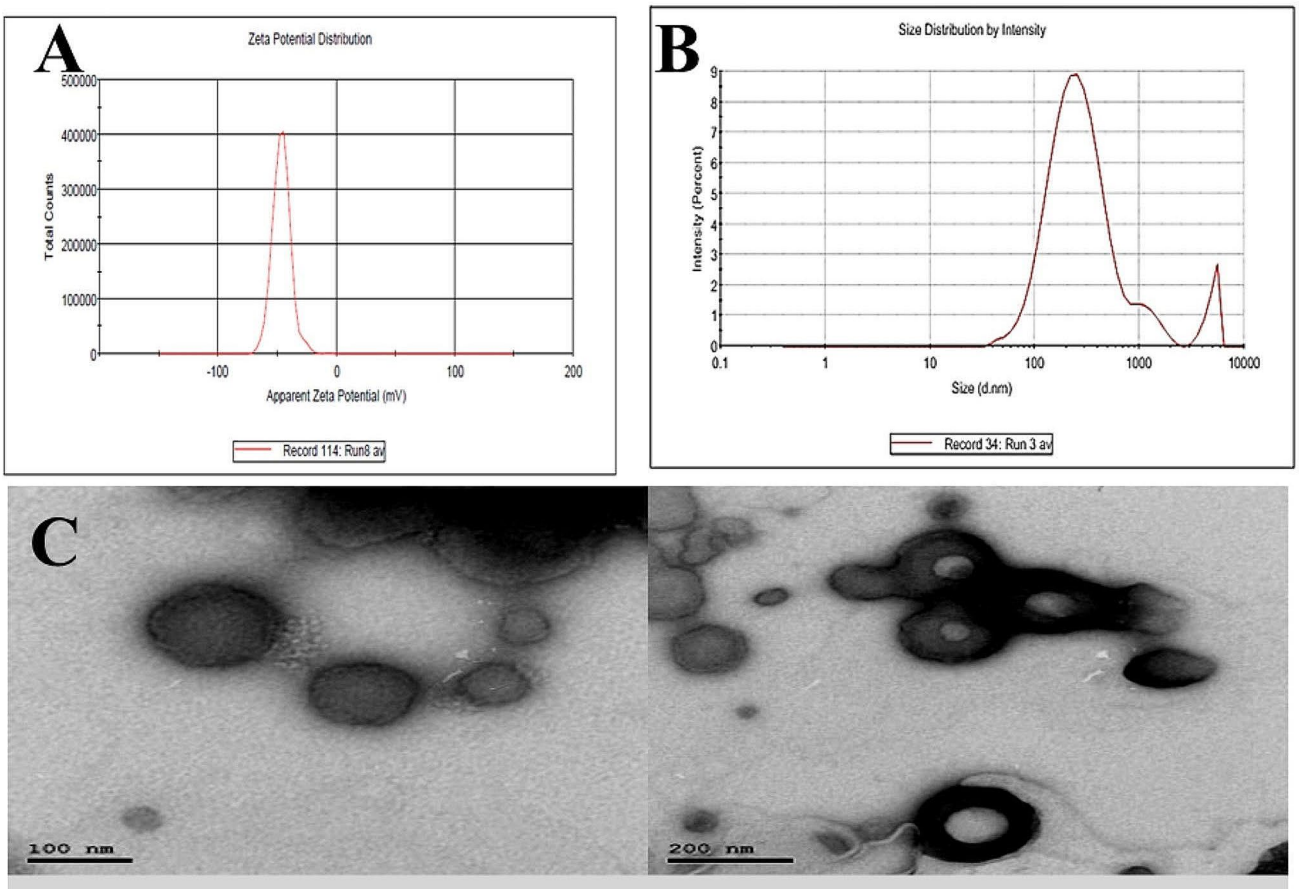

Fig. 5 (**A** and **B**) Zeta potential and particle size of fluconazole niosmal optimized formula (**C**)TEM of fluconazole niosmal optimized formula

Also, the chosen formula showed a PDI of 0.11 ± 0.09 indicating the homogeneity of the chosen formula.

Transmission electron Microscopy (TEM)

The selected formula morphology is shown in Fig. 5. Flu-Nio-laden contact lenses have a smooth well-defined sphere shape with a relatively uniform size distribution and a definite wall with an aqueous core. Flu-Nio-laden contact lens size obtained from the TEM examination agreed with the PS analysis and it showed a uniform size distribution.

Cytotoxicity Test

The cytotoxicity of the optimized formula Flu- Nio, Flu solution, and control were performed to demonstrate their effect on Mouse endothelial cells. The results revealed that Flu- Nio, Flu solution at a concentration of 10 µg/ml, and the control have a cell viability % of 99.22, 99.67, and 100% respectively, with no statistically significant difference detected. These results indicate that Flu- Nio, Flu solution at a concentration of 10 µg/ml had no harmful impact on normal Mouse endothelial cells as shown in Fig. 6. According to cytotoxicity test results, Flu-Nio is biocompatible and has low cytotoxicity. Fluconazole contact lenses showed non-significant variation in the loaded Flu concentration after soaking at both 4 and 7 days at $p < 0.001$.

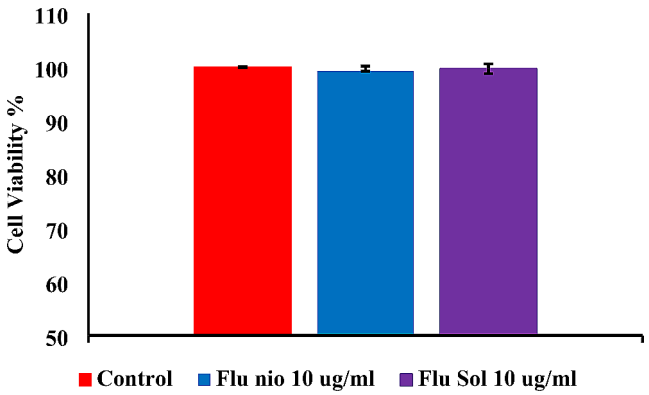

Fig. 6 Cytotoxicity profile of the optimized Flu-Nio, Flu solution, (at a concentration of 10 µg/ml) and control on C-166: Mouse Endothelial Cell after 24 h exposure to the Flu-Nio. Cytotoxicity test was done using sulforhodamine B (SRB) (0.4% w/v) and is represented as the cell viability percentage after applying the treatment

Fluconazole Quantification in the Contact Lenses

The concentration of Flu up taken in the contact lenses was assessed at different time intervals (at 4 days and 7 days) to show the maximum drug loaded. The results showed each contact lens contained 3.02 ± 0.23 and $3.11 \pm .081$for both 4 and 7 days respectively.

Light Transmission

The free contact lenses were clear and transparent; their light transmission measured at 600 nm showed a high transmission of $95.65 \pm 0.55\%$. The incorporation of Flu-Nio did lower the transmission to $90.743 \pm 0.47\%$ with no significant difference at ($p > 0.05$) with the free contact lenses because the nanosized particles diffract and scatter the incident lights [6]. The use of contact lenses with that amount of Flu-Nio would not affect the vision of the wearer which is essential [67].

In vitro Release of Fluconazole from (Flu-Nio) Laden Contact Lenses

In-vitro cumulative release of fluconazole from the optimized (Flu-Nio) laden contact lenses was compared with free drug solution and the results are shown in Fig. 7. The fluconazole from Flu- Nio-laden contact lenses was released and showed an initial burst release in the first hour (27.2% at 1 h), then it showed a prolonged release up to 48–72 h with a cumulative release of 79.62%. In contrast, the release of fluconazole from the control solution showed a high burst release in the first hour (46.4% at 1 h) and a 100% cumulative drug release after three hours. In addition, Flu-Nio is an efficient fluconazole carrier. The initial phase release of fluconazole from Flu-Nio-laden contact lenses could be attributed to free fluconazole penetration and drug desorption from the niosome surface. Free drug solution exhibited a significant ($P < 0.05$) higher and faster release than that from optimized Flu-Nio-laden contact lenses which may be attributed to the cholesterol of noisome that decreases the leakage of encapsulating fluconazole by reducing the niosomal membrane fluidity [68]. The results suggest that niosomes could be used to extend the release of fluconazole. According to the higher correlation coefficient, the drug release from the optimized Flu-Nio-laden contact lenses is best fitted to Baker and Lonsdale equation, indicating that fluconazole release from the vesicles could be attributed to the diffusion mechanism [69].

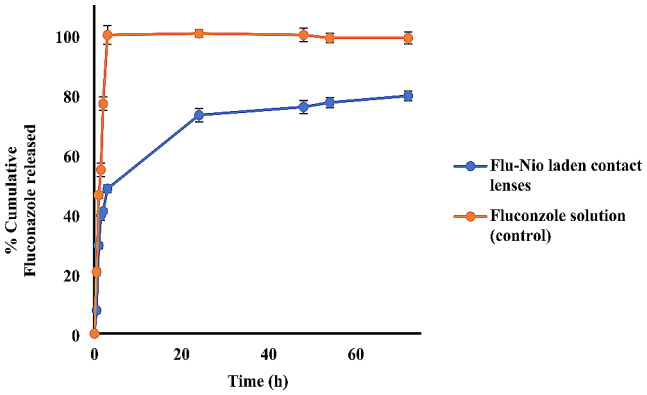

Fig. 7 Percentage cumulative release of fluconazole from Flu-Nio-laden contact lenses and fluconazole solution in simulated tear fluid (pH 6) at 37ºC ($n = 3$, mean ± standard deviation)

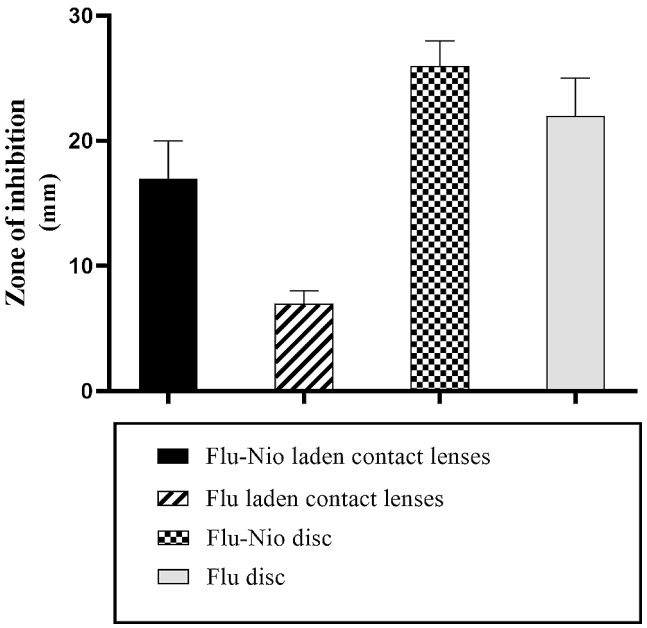

Fig. 8 Shows the zone of inhibition of Flu-Nio laden contact lenses, Flu-laden contact lenses, Flu-Nio disc, and Flu disc on *C. albicans* (ATCC® 10231), the growth inhibition was measured in mm after overnight incubation at 37 °C. Each experiment was done in triplicates, and an average data set is shown

Antimicrobial Activity Study

Antifungal Susceptibility by Disc Diffusion Method

Figure 8 shows the zone of inhibition of Flu-Nio-laden contact lenses (contact lens impregnated with Flu-Nio), Flu laden contact lenses (contact lens impregnated with Flu solution) and, Flu-Nio disc (sterile filter paper disc impregnated with Flu-Nio) and Flu disc (sterile filter paper disc impregnated with Flu solution) on *C. albicans* (ATCC® 10231). Flu-Nio-laden contact lenses and Flu-Nio disc increased the diameter of the zone of inhibition and showed

an increase in antifungal activity. Ciolino et al., 2011 [70] suggested that econazole-releasing contact lenses made of econazole-PLGA film encased within a pHEMA hydrogel preserved their fungicidal effects for three weeks. In addition, the formulation provides an alternate treatment for fungal keratitis and serves as a platform for ocular medication delivery. When designing a contact lens for antifungal ocular drug delivery, Phan and colleagues demonstrated that some aspects should be considered, such as (a) increasing the drug amounts to be loaded or released from the contact lenses; (b) the drug release rate from the contact lenses; and (c) consistent release with known concentration. The qualities of the lens material, the properties of the target drug, and the interactions between the polymer and the drug on the lens all have a substantial impact on the drug's uptake and release [71]. Previous research suggested that medications with a higher water solubility, such as fluconazole, might partition more quickly into aqueous systems. Furthermore, this causes fast drug release from the contact lenses, as seen with several ophthalmic medicines.

Determination of the Fungal Adhesion

Figure 9 shows the adherence of *C. albicans* on Flu-Nio-laden contact lenses compared with Flu-laden contact lenses, and the control lenses. The number of viable cells that could be cultivated after being released from the surface of contact lenses is used for measuring adhesion. Adhesion was reduced for both Flu-Nio and Flu-laden contact lenses. The 1×10^3 cells/ml that were initially added to the control lenses had increased to 8.3 ± 0.74 log CFU/lens on the lenses after the culture. Figure 9 shows that there was almost a 2 log-fold reduction of cell adherence to Flu-Nio-laden contact lenses compared with only a 1 log-fold reduction of cell adherence to Flu-laden contact lenses.

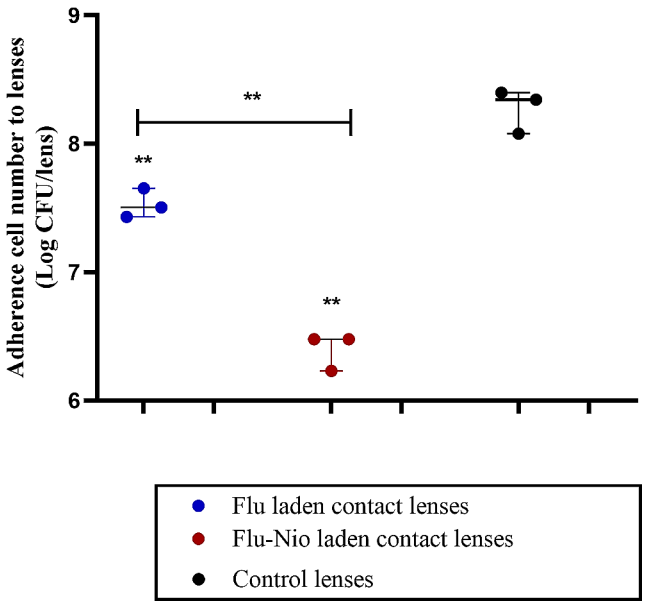

Fig. 9 Shows the effect on *Candida albicans* adhered to Flu-Nio-laden CL and Flu-laden CL, compared to that attached to control lenses. Adhesion, measured as the number of culturable viable cells after release from the lens surface, was reduced for both treated contact lenses compared to control lenses. The viability of adhered cells is represented as a median with an interquartile range after overnight incubation at 37 °C. Each experiment was done in three different cultures, and an average data set was taken. Statistical analysis was done using the student's t-test

Statistical analysis using student's t-test showed that there was a significant difference between the adhesion of *C. albicans* on Flu-Nio laden contact lenses and Flu-laden contact lenses compared with the control lenses ($P < 0.01$) and showed that Flu-Nio laden contact lenses had significantly lower fungal adherence than Flu laden contact lenses. This reduction in the fungal adhesion may be attributed to the small-sized Flu noisome which slowly diffuses Flu and acts by interacting with lanosterol 14-α demethylase, a cytochrome P-450 enzyme that converts lanosterol to ergosterol (essential for the fungal cell membrane) when its synthesis is suppressed, cells become more permeable and their contents pass out [33, 72, 73].

Determination of the Remaining C. *Albicans* in the Solution

The number of *C. albicans* cells in the PBS (pH) around the lenses throughout incubation was also measured (Fig. 10). The count of CFU per 1 mL of PBS after 24 h incubation surrounding the control lens was 8.5 ± 0.72 log CFU/lens. Flu-Nio-laden contact lenses showed a 2 log-fold reduction of cell number compared with Flu-laden contact lenses that showed only a 1 log-fold reduction of cell growth. These results indicate that during incubation, the drug was released into the fluid around the lenses and was effective against *C. albicans*. Statistical analysis using student's t-test showed that there was a significant difference between the remaining viable cells in the surrounding solution of Flu-Nio-laden contact lenses and Flu-laden contact lenses in comparison with control lenses ($P < 0.0001$) and showed that Flu-Nio laden contact lenses significantly reduced the microbial viable count than Flu laden contact lenses ($P < 0.001$). This could be attributed to the low diffusion of the Flu from the Flu-laden contact lens through the media. On the contrary, niosomes had resulted in better diffusion of the Flu from Flu-Nio-laden contact lenses, with a reduction in the fungal adhesion. The reason may be attributed to the small, lipophilic nature, and abundance of non-ionic surfactants [74]. Previous studies conducted by Willcox and co-workers found that the bacterial viability and adhesion for the tested strains was reduced by > 5 log reduction in solution or on

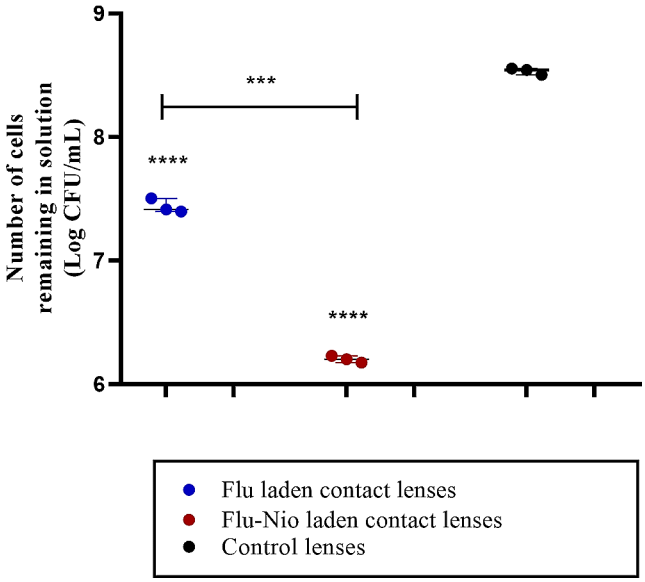

Fig. 10 Shows the effect on *C. albicans* remaining viable cells in the solutions surrounding Flu-Nio-laden CL and Flu-laden CL, compared to that surrounding the control lenses. The viability of adhered cells is represented as a median with an interquartile range after overnight incubation at 37 °C. Each experiment was done in three different cultures, and an average data set was taken. Statistical analysis was done using a student's t-test where statistical significance is represented by ***$P < 0.001$ and **** $P < 0.0001$

the lens surface using silver (20 ppm) nanoparticles lenses [42].

Conclusion

This work reveals that there is no interaction between the fluconazole, excipients, and their physical mixture. The optimized fluconazole noisome was developed and the particles attained a smooth spherical shape with uniform size distribution. The cytotoxicity test showed no harmful impact on normal mouse endothelial cells at a concentration of 10 µg/ml. The performance of the light transmission test for both free and Flu-Nio-laden contact lenses shows no significant difference and does not affect the contact lens visibility. The ability of fluconazole noisome-laden contact lenses to control drug release was noticed. Fluconazole from Flu-Nio-laden contact lenses was released and showed an initial burst release in the first hour, then it showed a prolonged release up to 72 h. Also, Flu-Nio-laden contact lenses synergize the inhibitory effect of fluconazole against the growth of C. albicans. In addition, Flu-Nio-laden contact lenses could reduce the fungal adhesion to their surface by C. albicans. These results demonstrated that Flu-Nio-laden contact lenses could be promising for delivering antifungals to treat fungal keratitis. An appropriate next step will be to investigate the Flu-Nio-laden contact lenses in a diseased animal model or an ex vivo model of candidal keratitis.

Acknowledgements Not applicable.

Funding Open access funding provided by The Science, Technology & Innovation Funding Authority (STDF) in cooperation with The Egyptian Knowledge Bank (EKB).

Data Availability All the relevant data are reported within the paper. For additional details, data are available on request to the authors.

Declarations

Conflict of Interest The authors declare that they have no known competing financial interests or personal relationships that could have appeared to influence the work reported in this article.

References

1. Ranch K, Patel H, Chavda L, Koli A, Maulvi F, Parikh RK. Development of in situ ophthalmic gel of dexamethasone sodium phosphate and chloramphenicol: a viable alternative to conventional eye drops. J Appl Pharm Sci. 2017;7(3):101–8.
2. Wadhwa S, Paliwal R, Paliwal SR, Vyas SP. Nanocarriers in ocular drug delivery: an update review. Curr Pharm Design. 2009;15(23):2724–50.
3. Gulsen D, Chauhan A. Ophthalmic drug delivery through contact lenses. Investig Ophthalmol Vis Sci. 2004;45(7):2342–7.
4. Hardberger R, Hanna C, Boyd CM. Effects of drug vehicles on ocular contact time. Arch Ophthalmol. 1975;93(1):42–5.
5. Ghate D, Edelhauser HF. Ocular drug delivery. Expert Opin Drug Deliv. 2006;3(2):275–87.
6. ElShaer A, Mustafa S, Kasar M, Thapa S, Ghatora B, Alany RG. Nanoparticle-laden contact lens for controlled ocular delivery of prednisolone: Formulation optimization using statistical experimental design. Pharmaceutics. 2016;8(2):14.
7. Urtti A. Challenges and obstacles of ocular pharmacokinetics and drug delivery. Adv Drug Deliv Rev. 2006;58(11):1131–5.
8. Gulsen D, Chauhan A. Dispersion of microemulsion drops in HEMA hydrogel: a potential ophthalmic drug delivery vehicle. Int J Pharm. 2005;292(1–2):95–117.
9. Xu J, Li X, Sun F. Cyclodextrin-containing hydrogels for contact lenses as a platform for drug incorporation and release. Acta Biomater. 2010;6(2):486–93.

10. Kim J, Conway A, Chauhan A. Extended delivery of ophthalmic drugs by silicone hydrogel contact lenses. Biomaterials. 2008;29(14):2259–69.
11. Mehta P, Al-Kinani AA, Arshad MS, Chang M-W, Alany RG, Ahmad Z. Development and characterisation of electrospun timolol maleate-loaded polymeric contact lens coatings containing various permeation enhancers. Int J Pharm. 2017;532(1):408–20.
12. Ciolino JB, Stefanescu CF, Ross AE, Salvador-Culla B, Cortez P, Ford EM, et al. In vivo performance of a drug-eluting contact lens to treat glaucoma for a month. Biomaterials. 2014;35(1):432–9.
13. Jung HJ, Abou-Jaoude M, Carbia BE, Plummer C, Chauhan A. Glaucoma therapy by extended release of timolol from nanoparticle loaded silicone-hydrogel contact lenses. J Controlled Release. 2013;165(1):82–9.
14. Costa VP, Braga MEM, Duarte CMM, Alvarez-Lorenzo C, Concheiro A, Gil MH, et al. Anti-glaucoma drug-loaded contact lenses prepared using supercritical solvent impregnation. J Supercrit Fluids. 2010;53(1–3):165–73.
15. Guzman-Aranguez A, Colligris B, Pintor J. Contact lenses: promising devices for ocular drug delivery. J Ocul Pharmacol Ther. 2013;29(2):189–99.
16. Chynn EW, Lopez MA, Pavan-Langston D, Talamo JH. Acanthamoeba keratitis: contact lens and noncontact lens characteristics. Ophthalmology. 1995;102(9):1369–73.
17. Schein OD, Glynn RJ, Poggio EC, Seddon JM, Kenyon KR, Microbial Keratitis Study G. The relative risk of ulcerative keratitis among users of daily-wear and extended-wear soft contact lenses. N Engl J Med. 1989;321(12):773–8.
18. Elmotasem H, Awad GEA. A stepwise optimization strategy to formulate in situ gelling formulations comprising fluconazole-hydroxypropyl-beta-cyclodextrin complex loaded niosomal vesicles and Eudragit nanoparticles for enhanced antifungal activity and prolonged ocular delivery. Asian J Pharm Sci. 2020;15(5):617–36.
19. Durak S, Esmaeili Rad M, Alp Yetisgin A, Eda Sutova H, Kutlu O, Cetinel S, et al. Niosomal drug delivery systems for ocular disease—recent advances and future prospects. Nanomaterials. 2020;10(6):1191.
20. Prabhu P, Kumar RN, Koland M, Harish NM, Vijayanarayan K, Dhondge G, et al. Preparation and evaluation of nano-vesicles of brimonidine tartrate as an ocular drug delivery system. J Young Pharmacists. 2010;2(4):356–61.
21. Marianecci C, Di Marzio L, Rinaldi F, Celia C, Paolino D, Alhaique F, et al. Niosomes from 80s to present: the state of the art. Adv Colloid Interface Sci. 2014;205:187–206.
22. Bayindir ZS, Yuksel N. Characterization of niosomes prepared with various nonionic surfactants for paclitaxel oral delivery. J Pharm Sci. 2010;99(4):2049–60.
24. Villate-Beitia I, Gallego I, Martínez-Navarrete G, Zárate J, López-Méndez T, Soto-Sánchez C, et al. Polysorbate 20 nonionic surfactant enhances retinal gene delivery efficiency of cationic niosomes after intravitreal and subretinal administration. Int J Pharm. 2018;550(1–2):388–97.
24. Carafa M, Santucci E, Lucania G. Lidocaine-loaded non-ionic surfactant vesicles: characterization and in vitro permeation studies. Int J Pharm. 2002;231(1):21–32.
25. Carafa M, Santucci E, Alhaique F, Coviello T, Murtas E, Riccieri FM, et al. Preparation and properties of new unilamellar non-ionic/ionic surfactant vesicles. Int J Pharm. 1998;160(1):51–9.
26. Kaur R, Mittal N, Kakkar M, Aggarwal AK, Mathur MD. Otomycosis: a clinicomycologic study. Ear nose Throat J. 2000;79(8):606–9.
27. Alnaim AS, Shah H, Nair AB, Mewada V, Patel S, Jacob S, et al. Qbd-based approach to optimize niosomal gel of levosulpiride for transdermal drug delivery. Gels. 2023;9(3):213.
28. Moraes RC, Carvalho AR, Lana AJD, Kaiser S, Pippi B, Fuentefria AM, et al. In vitro synergism of a water insoluble fraction of Uncaria tomentosa combined with fluconazole and terbinafine against resistant non-candida albicans isolates. Pharm Biol. 2017;55(1):406–15.
29. Oliveira MB, Calixto G, Graminha M, Cerecetto H, González M, Chorilli M. Development, characterization, and in vitro biological performance of fluconazole-loaded microemulsions for the topical treatment of cutaneous leishmaniasis. Biomed Res Int. 2015;2015.
30. Chen S, Hanning S, Falconer J, Locke M, Wen J. Recent advances in non-ionic surfactant vesicles (niosomes): fabrication, characterization, pharmaceutical and cosmetic applications. Eur J Pharm Biopharm. 2019;144:18–39.
31. Sambhakar S, Paliwal SK, Sharma S, Sati B, Singh B. Formulation and development of risperidone loaded niosomes for improved bioavailability: in vitro and in vivo study. Acta Pol Pharm–Drug Res. 2017;74:1859–73.
32. Attia IA, El-Gizawy SA, Fouda MA, Donia AM. Influence of a niosomal formulation on the oral bioavailability of acyclovir in rabbits. AAPS PharmSciTech. 2007;8:206–12.
33. El-Enin ASMA, Khalifa MKA, Dawaba AM, Dawaba HM. Proniosomal gel-mediated topical delivery of fluconazole: development, in vitro characterization, and microbiological evaluation. J Adv Pharm Tech Res. 2019;10(1):20.
34. Serramito Blanco M, Mota AF, Carpena Torres C, Huete Toral F, Álvarez, Lorenzo CI. Carracedo Rodríguez JG. Melatonin-eluting contact lenses effect on tear volume: In Vitro and In Vivo experiments. 2020.
35. Skehan P, Storeng R, Scudiero D, Monks A, McMahon J, Vistica D, et al. New colorimetric cytotoxicity assay for anticancer-drug screening. JNCI: J Natl Cancer Inst. 1990;82(13):1107–12.
36. Allam RM, Al-Abd AM, Khedr A, Sharaf OA, Nofal SM, Khalifa AE, et al. Fingolimod interrupts the cross talk between estrogen metabolism and sphingolipid metabolism within prostate cancer cells. Toxicol Lett. 2018;291:77–85.
37. Manosroi A, Chankhampan C, Ofoghi H, Manosroi W, Manosroi J. Low cytotoxic elastic niosomes loaded with salmon calcitonin on human skin fibroblasts. Hum Exp Toxicol. 2013;32(1):31–44.
38. Huang J-F, Zhong J, Chen G-P, Lin Z-T, Deng Y, Liu Y-L, et al. A hydrogel-based hybrid theranostic contact lens for fungal keratitis. ACS Nano. 2016;10(7):6464–73.
39. Maulvi FA, Choksi HH, Desai AR, Patel AS, Ranch KM, Vyas BA, et al. pH triggered controlled drug delivery from contact lenses: addressing the challenges of drug leaching during sterilization and storage. Colloids Surf B. 2017;157:72–82.
40. CLSI. Clinical and Laboratory Standards Institute. Performance Standards for Antimicrobial Susceptibility Testing; Twenty-First Informational Supplement. CLSI Document M100-S21 Wayne, PA. 2020.
41. Sonoyama H, Araki-Sasaki K, Kazama S, Kawasaki T, Ideta H, Sunada A, et al. The characteristics of keratomycosis by Beauveria Bassiana and its successful treatment with antimycotic agents. Clin Ophthalmol (Auckland NZ). 2008;2:675–8.
42. Willcox MDP, Hume EBH, Vijay AK, Petcavich R. Ability of silver-impregnated contact lenses to control microbial growth and colonisation: J Optom. 2010;3(3):143-8. https://doi.org/10.1016/S1888-4296(10)70020-0. Epub 2010 Dec 7.; 2011.
43. Mosdam T. Rapid colorimetric assay for cellular growth and survival: application to proliferation and cytotoxic assay. J Immunol Methods. 1983;65:55–63.
44. Fatima I, Rasul A, Shah S, Saadullah M, Islam N, Khames A, et al. Novasomes as nano-vesicular carriers to enhance topical delivery of fluconazole: a new approach to treat fungal infections. Molecules. 2022;27(9):2936.

45. Farmoudeh A, Akbari J, Saeedi M, Ghasemi M, Asemi N, Nokhodchi A. Methylene blue-loaded niosome: preparation, physicochemical characterization, and in vivo wound healing assessment. Drug Delivery Translational Res. 2020;10:1428–41.
46. Fatehi P, Baba AS, Eh Suk VR, Misran M. Preparation and characterization of palm oil in water microemulsion for application in the food industry. Br Food J. 2020;122(10):3077–88.
47. Miatmoko A, Safitri SA, Aquila F, Cahyani DM, Hariawan BS, Hendrianto E, et al. Characterization and distribution of niosomes containing ursolic acid coated with chitosan layer. Res Pharm Sci. 2021;16(6):660.
48. Akay S, Kayan B. Aqueous solubility and chromatographic studies of antifungal drug-fluconazole at high temperature conditions. J Mol Liq. 2021;328:115438.
49. Abd-Elal RMA, Shamma RN, Rashed HM, Bendas ER. Transnasal zolmitriptan novasomes: in-vitro preparation, optimization and in-vivo evaluation of brain targeting efficiency. Drug Delivery. 2016;23(9):3374–86.
50. Yasam VR, Jakki SL, Natarajan J, Venkatachalam S, Kuppusamy G, Sood S, et al. A novel vesicular transdermal delivery of nifedipine–preparation, characterization and in vitro/in-vivo evaluation. Drug Delivery. 2016;23(2):619–30.
51. El-Ridy MS, Yehia SA, Mohsen AM, El-Awdan SA, Darwish AB. Formulation of niosomal gel for enhanced transdermal lornoxicam delivery: in-vitro and in-vivo evaluation. Curr Drug Deliv. 2018;15(1):122–33.
52. Modha NB, Chotai NP, Patel VA, Patel BG. Preparation, characterization and evaluation of fluconazole polymorphs. Int J Res Pharm Biomed Sci. 2010;1(2):124–7.
53. Hashemic SMH, AmirhosseinBabaeic SM. Curcumin Niosomes (curcusomes) as an alternative to conventional vehicles: A potential for efficient dermal delivery.
54. Demirbolat GM, Aktas E, Coskun GP, Erdogan O, Cevik O. New approach to formulate methotrexate-loaded niosomes: in vitro characterization and cellular effectiveness. J Pharm Innov. 2021:1–16.
55. El-Far SW, Abo El-Enin HA, Abdou EM, Nafea OE, Abdelmonem R. Targeting colorectal cancer cells with niosomes systems loaded with two anticancer drugs models; comparative in vitro and anticancer studies. Pharmaceuticals. 2022;15(7):816.
56. Shehata TM, Ibrahim MM, Elsewedy HS. Curcumin niosomes prepared from proniosomal gels: in vitro skin permeability, kinetic and in vivo studies. Polymers. 2021;13(5):791.
57. Taymouri S, Varshosaz J. Effect of different types of surfactants on the physical properties and stability of carvedilol nano-niosomes. Adv Biomedical Res. 2016;5.
58. Emad Eldeeb A, Salah S, Ghorab M. Proniosomal gel-derived niosomes: an approach to sustain and improve the ocular delivery of brimonidine tartrate; formulation, in-vitro characterization, and in-vivo pharmacodynamic study. Drug Delivery. 2019;26(1):509–21.
59. Teaima MH, Abdelnaby FA, Fadel M, El-Nabarawi MA, Shoueir KR. Synthesis of Biocompatible and environmentally nanofibrous mats loaded with moxifloxacin as a Model Drug for Biomedical Applications. Pharmaceutics. 2020;12(11):1029.
60. Essa EA. Effect of formulation and processing variables on the particle size of sorbitan monopalmitate niosomes. Asian J Pharm (AJP). 2010;4(4).
61. Moriyama E, Saito T, Tokuoka Y, Takeuchi S, Kawashima N. Evaluation of the hardness of lipid bilayer membranes of liposomes by the ultrasound attenuation method. J Oleo Sci. 2003;52(8):433–7.
62. Waqas MK, Sadia H, Khan MI, Omer MO, Siddique MI, Qamar S, et al. Development and characterization of niosomal gel of fusidic acid: In-vitro and ex-vivo approaches. Des Monomers Polym. 2022;25(1):165–74.
63. Kumar YP, Kumar KV, Kishore VS. Preparation and evaluation of diclofenac niosomes by various techniques. Res J Pharm Technol. 2013;6(10):1097–101.
64. Mujeeb SA, Sailaja AK. Formulation of ibuprofen loaded niosomal gel by different techniques for treating rheumatoid arthritis. J Bionanosci. 2017;11(3):169–76.
65. Estupiñan OR, Garcia-Manrique P, Blanco-Lopez MC, Matos M, Gutiérrez G. Vitamin D3 loaded niosomes and transfersomes produced by ethanol injection method: identification of the critical preparation step for size control. Foods. 2020;9(10):1367.
66. Ammar HO, Haider M, Ibrahim M, El Hoffy NM. In vitro and in vivo investigation for optimization of niosomal ability for sustainment and bioavailability enhancement of diltiazem after nasal administration. Drug Delivery. 2017;24(1):414–21.
67. Maulvi FA, Desai AR, Choksi HH, Patil RJ, Ranch KM, Vyas BA, et al. Effect of surfactant chain length on drug release kinetics from microemulsion-laden contact lenses. Int J Pharm. 2017;524(1–2):193–204.
68. Fetih G. Fluconazole-loaded niosomal gels as a topical ocular drug delivery system for corneal fungal infections. J Drug Deliv Sci Technol. 2016;35:8–15.
69. Baker RW. Controlled release: mechanisms and rates. Controlled Release Biologically Act Agents. 1974;15.
70. Ciolino JB, Hudson SP, Mobbs AN, Hoare TR, Iwata NG, Fink GR, et al. A prototype antifungal contact lens. Invest Ophthalmol Vis Sci. 2011;52(9):6286–91.
71. Phan CM, Bajgrowicz M, McCanna DJ, Subbaraman LN, Jones L. Effects of Antifungal soaked silicone hydrogel contact lenses on Candida albicans in an Agar Eye Model. Eye Contact Lens. 2016;42(5):313–7.
72. Fritsch LN, Dias ALT, Silva NC, Fernandes GJM, Ribeiro FBAO. Comparative analysis of biofilm formation by < i > Candida albicans and < i > Candida krusei in different types of contact lenses. Arquivos brasileiros de oftalmologia. 2022;85.
73. Zhu B, Li Y, Mei W, He M, Ding Y, Meng B, et al. Alogliptin improves endothelial function by promoting autophagy in perivascular adipose tissue of obese mice through a GLP-1-dependent mechanism. Vascul Pharmacol. 2019;115:55–63.
74. Kattar A, Quelle-Regaldie A, Sánchez L, Concheiro A, Alvarez-Lorenzo C. Formulation and characterization of Epalrestat-Loaded Polysorbate 60 Cationic niosomes for Ocular Delivery. Pharmaceutics. 2023;15(4):1247.